Carbohydrate Polymers 89 (2012) 290–297

Contents lists available at SciVerse ScienceDirect

Carbohydrate Polymers

journal homepage: www.elsevier.com/locate/carbpol

Effect of crosslinker and nanoclay on starch and jute fabric based green nanocomposites

Murshid Iman, Tarun K. Maji*

Department of Chemical Sciences, Tezpur University, Assam 784028, India

ARTICLE INFO

Article history:
Received 13 January 2012
Received in revised form 23 February 2012
Accepted 3 March 2012
Available online 8 March 2012

Keywords:
Starch
Jute
Nanoclay
Glutaraldehyde
Green nanocomposite

ABSTRACT

'Green' nanocomposites were prepared by solution induced intercalation method using starch, jute, glutaraldehyde, nanoclay and glycerol. The concentration of glycerol was optimised. The synthesized composites were characterized by various physicochemical and spectrochemical techniques such as Fourier transform infrared spectroscopy, X-ray diffractometry, transmission electron microscopy, scanning electron microscopy, and thermogravimetric analysis. Fourier transform infrared spectroscopy study indicated an interaction between the jute, starch and clay. Good adhesion exists between starch and jute surface as revealed by scanning electron microscope study. The extent of exfoliation of clay was studied by X-ray diffraction and transmission electron microscope studies. The addition of glutaraldehyde and nanoclay has been found to improve the thermal stability, flame retardancy, dimensional stability and mechanical strength of the prepared composite.

1. Introduction

The growing awareness of the pressing need for greener, more sustainable technologies has focussed attention on use of ecofriendly and cost-effective material with high performance (Ma, Yu, & Kennedy, 2005). Another aspect, which is receiving more attention, is the use of alternate source prior to the use of the conventional materials (Satyanarayana, Arizaga, & Wypych, 2009). Biopolymers, which exist abundantly worldwide, are one of such promising material. They offer many fundamental and practical advantages of relevance to the chemist as well as to the chemical industries, which are constantly searching for high performing, cost-effective and environmentally friendly materials (Bastioli, 1995; Pandey & Singh, 2001; Scott, 2000; Shogren, Fanta, & Doanne, 1993). Besides these, natural fibres with their characteristics properties such as low cost, easy availability, low density, high specific strength, renewability and less abrasive with respect to processing tools, can be added to such class of materials (Ray, Sengupta, Sengupta, Mohanty, & Misra, 2007; Saheb & Jog, 1999). Among various natural fibres, jute fibre is cheap and widely available (especially in some Asian countries) (Ray & Sarkar, 2001). Jute, mainly comprising of cellulose and lignin, is an extensively demanding materials in cloth and other such industries (Jahan, Saeed, He, & Ni, 2011; Saha, Das, Basak, Bhatta, & Mitra, 2000). Therefore, with the use of greener methodologies and environmentally benign materials (such as biopolymers), jute can be modified to a cost-effective and environmentally friendly 'green' products with improved physical properties (Plackett, Anderson, Pedersen, & Nielson, 2003).

One of the most studied and promising raw materials for the production of biodegradable products is starch, a natural, renewable carbohydrate and low cost polymer obtained from a great variety of crops such as corn, wheat, rice and potato (Corre, Bras, & Dufresne, 2010). Starch is basically a mixer of amylose, a linear polymer with molecular weight between 103 and 106 and amylopectin, a branched polymer with a —(1–6)— linked branch points (Dufrense & Vignon, 1998). Native starch commonly exists in a granular structure with about 15–45% crystallinity. Under the action of high temperature and shear, starch can be processed into thermoplastic starch (Forssell, Mikkilä, Moates, & Parker, 1997). Starch based films have significant potential to replace synthetic films such as polyethylene in packaging and agricultural mulching industries (Chen & Patel, 2012). Starch has been investigated widely for the potential manufacture of medical delivery systems and devices (Fishman, Coffin, Konstance, & Onwulata, 2000). However, starch based films have limited applications due to their two main disadvantages such as high hydrophilicity and inherently low moduli of elasticity (Ban, JianguoSong, Argyropoulos, & Lucia, 2006).

Polymer–layered silicate nanocomposites, containing small amounts of inorganic nano phase, have exhibited superior properties like modulus, strength, thermal stability, toughness, gas permeability barrier, and flammability resistance compared to those of the pure polymers (Yoonessi, Toghiani, Kingery, & Pittman, 2004). These unique properties shown by nanocomposites are due

* Corresponding author. Tel.: +91 3712 267007x5053; fax: +91 3712 267005.
E-mail address: tkm@tezu.ernet.in (T.K. Maji).

0144-8617/$ – see front matter © 2012 Elsevier Ltd. All rights reserved.
doi:10.1016/j.carbpol.2012.03.012

to the nanometric size effect, compared to conventional composite even at low nanofiller content (Bondeson, Mathew, & Oksman, 2006). Therefore, the use of such material can play a vital role in improving the properties of composites based on biopolymers. Among all the potential nanocomposites predecessors, montmorillonite clay is most commonly used layered silicates for the preparation of nanocomposites. The use of nanoclay in various organic synthesis and other industry has been known for many years (Gao, Dong, Hou, & Zhang, 2012; Mitsudome et al., 2012; Sukitpaneenit & Chung, 2012; Zhang et al., 2012). However, their applications along with the renewable resources have not been explored fully and in recent year there has been considerable interest in the use of nanoclay for improvising the properties of biocomposites (Ray & Okamoto, 2003).

In this study, we have prepared composites by using starch, jute and glutaraldehyde (GA). The composites have been prepared by varying the amount of GA from 30 to 70% and keeping other components (starch, jute and glycerol) constant. The effect of the crosslinker, i.e. GA on the physiochemical properties such as mechanical, thermal and dimensional stability have been studied by various techniques. The composites have further been modified by addition of different amount of nanoclay and their effects on various properties of the composites stated above have been studied.

2. Experimental

2.1. Materials

Jute fabrics (0.450 g cm^{-2}) were purchased from local market, Tezpur, Assam, India. Starch soluble extra pure, glutaraldehyde 25% (w/v), benzene (purity > 99%) and NaOH (purity > 97%) pellets used for this study were obtained from Merck Private Limited (Mumbai, India). Glycerol (AR grade) and montmorillonite K-10 clay (purity 99.99%) were obtained from Qualigens Fine Chemicals, (Mumbai) and Sigma–Aldrich (USA), respectively. All other chemicals received as such were used without any further treatment.

3. Methods

3.1. Surface modification of jute

Jute fabrics (J) were first treated with 2% liquid detergent (Rankleen M/S Rankem, India; pH: 6.5–7.5) at 70 °C for 1 h, then washed with distilled water and finally dried in a vacuum oven at 70 °C till attainment of constant weight. The washed fabrics were dewaxed by treatment with a mixture of alcohol and benzene (1:2) for 72 h at 50 °C. It was washed with distilled water and dried till attainment of constant weight. The fabrics were then treated with 5% (w/v) NaOH solution for 30 min at 30 °C, and washed with distilled water for several times to leach out the absorbed alkali. The fabrics were finally kept immersed in distilled water for overnight and were washed repeatedly to avoid the presence of any trace amount of alkali. The alkali treated fabrics were dried in a vacuum oven at 70 °C to constant weight and stored at ambient temperature in a desiccator.

3.2. Preparation of the slurry

To process starch powder into a suitable resin for fabricating 'green' composites, it was mixed thoroughly with deionized water at 1:10 ratio (by w/w) and stirred continuously. Starch was found to be very brittle, weak and difficult to process into useful films in absence of plasticizer. Therefore, glycerol was added as a plasticizer. The optimum amount of glycerol required to process starch into useful film was 5% (w/w of dry starch). The slurry containing starch and glycerol (5%, w/w) was transferred to a 500 ml round bottom flask and stirred with a mechanical stirrer maintaining the temperature in the range 55–60 °C for 4 h. The temperature of the slurry was then cooled to 35 °C. To this, glutaraldehyde (GA) was added and stirred for another 5 min at that temperature. The amount of GA was varied from 30 to 70% (w/w of dry starch). This stage is referred to as pre-cured resin. In order to prepare clay filled resin, desired amount of clay (1–5% (w/w of dry starch)) was first taken in a beaker containing water, stirred for 6 h using mechanical stirrer followed by sonication for 30 min under 0.5 cycle and a wave amplitude of 140 μm using a sonicator (Heilscher UP200S, Germany) and finally added to the pre-cured resin.

3.3. Impregnation of jute fabrics and fabrication of the composite

The pre-cured resin was then poured in a bowl and the surface modified jute fabric was dipped into the resin slurry for 24 h at ambient temperature (25 °C). The impregnated jute fabrics were placed in a Teflon coated glass plate and dried over a heating plate at 30–40 °C for 12 h. The weight of the jute fabrics was noted before impregnation (W_1).

Composite laminates were prepared by the method of film stacking. The layers of impregnated jute fabric were placed on one another on 15 levels in a metal mould of thickness 3 mm. The laminates were then compression moulded in a compression moulding press (Santec, New Delhi) at 80 °C under a pressure of 100 MPa. The laminates were 3 mm in thickness. The final weight of the composite was noted (W_2). The calculations were made as per the following equations:

$$\text{Percentage of Jute in the composite} = \left(\frac{W_1}{W_2}\right) \times 100 \quad (1)$$

$$\text{Percentage of resin in the composite} = \left\{\frac{(W_2 - W_1)}{W_2}\right\} \times 100 \quad (2)$$

where W_1 = weight of jute fabrics before impregnation and W_2 = weight of the final composite.

4. Measurements

4.1. Fourier transform infrared spectroscopy (FT-IR)

FT-IR spectra of the post-cured composite samples were recorded in FTIR Nicolet, Impact 410 spectrophotometer, USA. Small quantities of finely powder composite samples were thoroughly grounded with exhaustively dried KBr and pellets were prepared by compression under vacuum.

4.2. X-ray diffractometry (XRD)

The XRD measurements were carried out in a Rigaku X-ray diffractometer (Miniflex, UK) using Cu Kα (λ = 0.154 nm) radiation at a scanning rate of 2° min^{-1} with an angle ranging from 2° to 30° to know the degrees of clay intercalation in composite.

4.3. Transmission electron microscopy (TEM)

The study of the dispersion of silicate layers of montmorillonite clay nanoparticles in jute reinforced starch composite was carried out by using Transmission Electron Microscope (JEOL, JEM 2100) at an accelerating voltage of 200 kV.

4.4. Scanning electron microscopy (SEM)

The surface morphology of some of the prepared samples was studied by scanning electron microscopy (SEM) before it was subjected to flexural test. The morphology of the fractured surface of the samples obtained from flexural test was also studied by SEM. The analysis was performed by using a JEOL scanning electron microscope (model JSM-6390LV) at an accelerating voltage of 5–15 kV. All of the samples were Pt coated before observation.

4.5. Thermogravimetric analysis (TGA)

Thermogravimetric analysis of the composite samples were done by using Shimazdu TGA 50, thermal analyzer under the nitrogen flow rate of 30 mL min^{-1} at the heating rate of 10 °C min^{-1} from 30 °C to 600 °C. The sample weight was approximately 5 mg. Three samples were tested of each set to obtain a constant value.

4.6. Mechanical property

The tensile properties of the composites were determined in accordance with ASTM D-638 at a crosshead speed of 2 mm min^{-1}. The samples were cut into blocks of 100 mm × 3 mm × 20 mm (longitudinal × radial × tangential). For the flexural test, the specimens were cut into dimension of 3 mm × 10 mm × 100 mm (radial × tangential × longitudinal) and examined as per ASTM D-790 at a crosshead speed of 2 mm min^{-1}. Both the tensile and flexural strength of the samples were measured by Universal Testing Machine-HOUNSEFIELD, England (model H100K-S) at room temperature. Five samples were tested for each set and the mean value was reported.

4.7. Limiting oxygen index (LOI)

Limiting oxygen index (LOI) is defined as the minimum concentration of oxygen, expressed as percent volume, in a flowing mixture of oxygen and nitrogen that will support flaming combustion of a material initially at room temperature. The specimens were cut into 100 mm × 6 mm × 3 mm (longitudinal × tangential × radial) according to ASTM-D 2863 and placed vertically in the flammability tester (S.C. Dey Co., Kolkata). The total volume of the gas mixture ($N_2 + O_2$) was kept fixed at 18 cc. The volume of nitrogen gas and that of oxygen gas were kept initially at a maximum and minimum level. Now, the volume of nitrogen gas was decreased and that of oxygen gas was increased gradually. However, the total volume of gas mixture was kept fixed at 18 cc during the experiment. The ratio of nitrogen and oxygen at which the sample continued to burn for at least 30 s was recorded.

$$\text{Limiting oxygen index (LOI)} = \left\{ \frac{\text{Volume of } O_2}{\text{Volume of } (O_2 + N_2)} \right\} \times 100$$

4.8. Dimensional stability

The synthesised composite were cut into blocks of 3 mm × 10 mm × 25 mm (radial × tangential × longitudinal) for dimensional stability test. Dimension of oven dried samples were measured and conditioned at room temperature (30 °C) and 30% relative humidity. The samples were then kept in humidity chamber at room temperature maintaining relative humidity of 65% for 72 h. The specimens were taken out from the humidity chamber after stipulated time period and volume were measured with the help of slide callipers. Swelling is considered as a change in volume and expressed as percentage of volume increase compared to oven dried samples. The percentage of swelling in water vapour was calculated as per formula given below:

$$\%\,\text{Swelling} = \left(\frac{V_t - V_0}{V_0} \right) \times 100$$

where 'V_t' is volume of the sample after "t" time and 'V_0' is initial volume of composite sample before water vapour absorption.

Table 1
Different composition of prepared composite.

Sample	Starch (wt.%)	Glycerol (wt.%)	GA (wt.%)	Jute (wt.%)	MMT (wt.%)
S/J	100	5	–	75	–
S/J/G30	100	5	30	75	–
S/J/G40	100	5	40	75	–
S/J/G50	100	5	50	75	–
S/J/G60	100	5	60	75	–
S/J/G70	100	5	70	75	–
S/J/G50/M1	100	5	50	75	1
S/J/G50/M3	100	5	50	75	3
S/J/G50/M5	100	5	50	75	5

5. Results and discussion

Preliminary investigations showed that the optimum percentage of glycerol required to process starch into useful film was 5% (w/w of dry starch) (data not shown). The samples, as coded in Table 1, had been prepared by keeping the weight (%) of the components viz. starch, glycerol and jute constant in all the samples where as the percentages (%) of GA and nanoclay were varied. The weight (%) of the various components used for the synthesis of the composite are provided in Table 1.

5.1. FTIR study

The interactions between starch, jute, glycerol, clay and glutaraldehyde were studied by FTIR spectroscopy. FTIR spectra of starch, jute, clay, S/J, S/J/GA and S/J/GA/M are presented in Fig. 1(A). The FTIR spectrum of starch (curve (a)) shows the presence of absorption bands at 571, 980, 1160, 1650, 2920 and 3400 cm^{-1} confirming the carbohydrate nature (Aboubakar, Njintang, Scher, & Mbofung, 2008). The typical saccharide bands appeared in the range 1180–950 cm^{-1} was considered as the vibration modes of C—C and C—O stretching and the bending of C—H bonds (Liu, Chaudhary, Yusa, & Tade, 2011). Jute (curve (b)) shows the presence of peaks in the range 3440–3390 cm^{-1} for —OH stretching, 1738 cm^{-1} for the C=O stretching vibration of ester groups of hemicelluloses, 1640 cm^{-1} for C=O stretching, 1254 cm^{-1} for —C—O—C— bond in cellulose chain and 1057–1116 cm^{-1} for C—O stretching. Clay exhibits (curve (c)) peaks at 3465 cm^{-1} (—OH stretching), 1619 cm^{-1} (—OH bending), 1030–460 cm^{-1} (oxide bonds of metals like Si, Al, Mg, etc.).

Characteristics peaks of starch and jute were appeared in the spectrum of S/J composite (curve (d)). Curve (e) represents the spectrum of glutaraldehyde crosslinked S/J composite. The intensities of —OH and C=O stretching were found to decrease in the crosslinked composites suggesting the formation of covalent bond between jute and starch. The possible interaction between starch, jute and glutaraldehyde are given in Fig. 1(B). In the spectrum of clay filled (curve (f)) S/J composites, the intensity of peak corresponding to —OH had further decreased. The intensities of peaks at 1620 cm^{-1} and 1030 cm^{-1} assigned for Si—O—Si stretching were more pronounced compared to glutaraldehyde crosslinked S/J composites. All this suggested the participation of hydroxyl group of clay in crosslinking reaction with starch and jute (Deka & Maji, 2011).

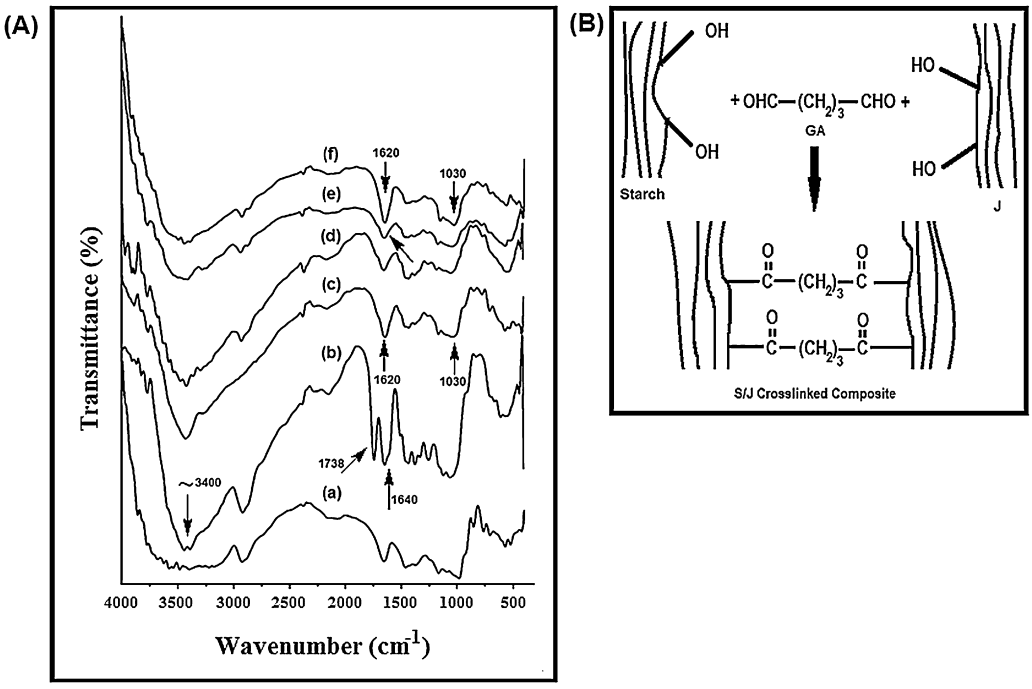

Fig. 1. (A) FTIR spectra of (a) starch, (b) jute, (c) clay, (d) S/J, (e) S/J/G50 and (f) S/J/G50/M5. (B) Schematic diagram of glutaraldehyde crosslinked starch/jute composite.

The FTIR spectra taken for samples with different concentrations of glycerol (not shown in Fig. 1(A)) did not produce neither any new peak nor any significant change in intensity of other peaks except the broadening of the —OH peak which is of course expected.

5.2. XRD study

The interlayer spacing (*d*-spacing) of the starch/nanoclay nanocomposites prepared via solution induced intercalation method was detected by X-ray diffraction study. Fig. 2(A) shows the XRD patterns of Jute, starch, S/J, S/J/G50, clay and the nanocomposites. Clay shows sharp peaks around $2\theta = 24^\circ$ and 9°. The peak around 9° corresponds to a *d*-spacing of about 1.2 nm in pure clay (Huang & Netravali, 2006). Jute shows peaks at $2\theta = 22^\circ$ (0 0 2 plane of cellulose I) and 19° (1 0 1 plane of cellulose II) (Kvien, Sugiyama, Votrubec, & Oksman, 2007). Curve (b) represents the diffractograms of starch. A little broader peak around $2\theta = 20^\circ$ was found to appear. Curves (c) and (d) representing the composites without and with crosslinker exhibited no diffraction peak between 1° and 10° in the 2θ range, reflecting the absence of any ordered structure of starch

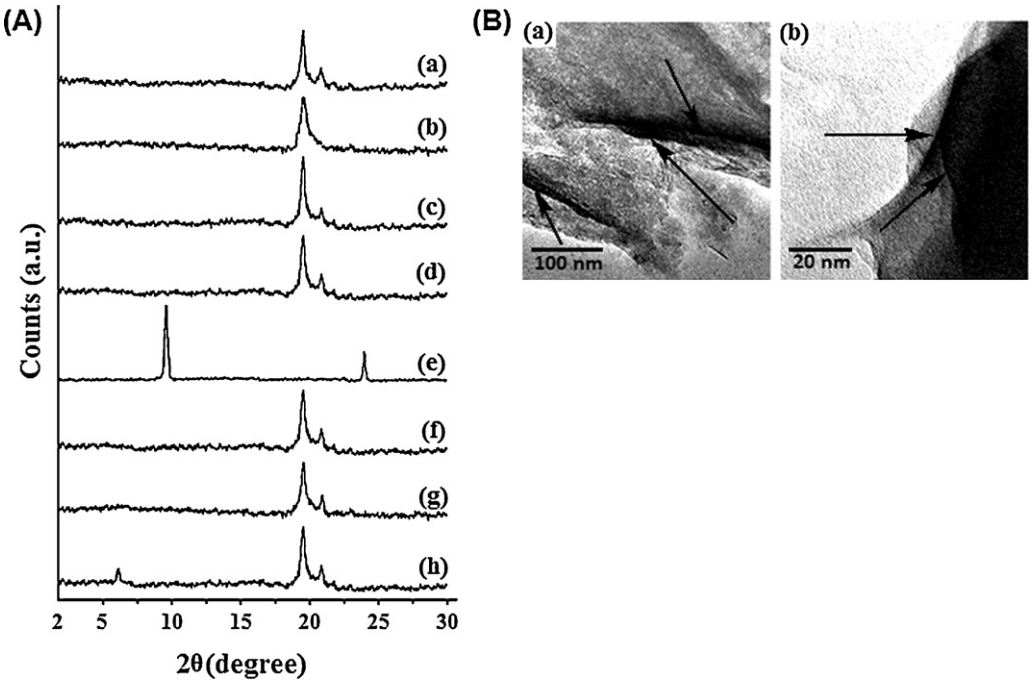

Fig. 2. (A) XRD patterns of (a) jute, (b) starch, (c) S/J, (d) S/J/G50, (e) clay, (f) S/J/G50/M1, (g) S/J/G50/M3 and (h) S/J/G50/M5. (B) TEM micrographs of S/clay composite with 5% clay (a) 100 nm and (b) 20 nm scale.

and jute in this range. The diffraction peak of the nanoclay tactoids was absent in the X-ray diffractograms for 1% and 3% clay loaded composites (curves (f) and (g)). It could be said that either the full expansion of the MMT gallery occurred, which was not possible to detect by XRD, or the MMT layers became delaminated and no crystal diffraction peak appeared (Lu, Zhao, & Xue, 2006). As shown in Fig. 2(A) (curve (h)), the peak obtained for pure clay at around 9° was shifted towards left with reduction in intensity in the S/J/G50/M5 composites. This indicated that the layer in clay was delaminated in the aqueous medium by the starch macromolecules (Chen & Zhang, 2006).

There was no characteristic change in the XRD pattern recorded for various samples prepared by treating with different concentrations of glycerol.

5.3. TEM study

TEM analysis was carried out to verify the extent of exfoliation of nanoclay in the synthesized composites. The dispersion of clay layers as dark lines (shown by arrow mark) was observed in both the images. The TEM micrographs of nanoclay incorporated composites are shown in Fig. 2(B). Fig. 2(B)-((a) and (b)) represent the TEM micrographs in 100 and 20 nm range. As indicated by TEM micrographs, the clay layers were delaminated into thin lamellas by starch having a dimension of 2–3 nm in thickness. This suggested that the nanoclay were well dispersed and partially exfoliated into starch matrix. This type of partially exfoliated structure of nanoclay was also reported in various literatures and had been considered as a successful intercalation of the nanoclay into the composites (Chen & Zhang, 2006; Yoonessi et al., 2004). Therefore, from XRD and TEM studies, it could be concluded that S/J/Clay nanocomposites with a delaminated structure could be prepared by solution induced intercalation method in neutral aqueous medium.

5.4. SEM study

SEM micrographs of jute, starch and the smooth surface and fractured surface of S/J composite without and with clay are presented in Fig. 3(A). The surface of jute fibres was smooth and regular (Fig. 3(A)-(a)). The shape of starch particles were irregular compact disc type as shown in Fig. 3(A)-(b) (Aboubakar et al., 2008). On addition of GA, S/J composite appeared rough (Fig. 3(A)-(c)) (Hillberg, Holmes, & Tabrizian, 2009). The roughness was increased with the addition of clay (Fig. 3(A)-(e)). The roughness might be due to the adherence of either the starch or the starch/clay to the jute surface. However, on addition of GA into the composite less fibres were found to be the protruded out of the composite (Fig. 3(A)-(d)). This suggested a failure in the brittleness of the starch matrix. The resins were found to adhere on some of the fibre surface. Surface of some fibres were smooth as there was no resin. Moreover, on addition of nanoclay into the composite, the brittleness was found to enhance (Fig. 3(A)-(f)). This might be due to the fact that the clay particles increased the interaction with starch matrix and jute fibre surface which resulted in less pull out of fibres from the fractured surface (Ray et al., 2007).

Further work was done through energy dispersive X-ray analysis of the nanoparticles observed in the fracture for the clay loaded composite as shown in Fig. 3(B). Elements such as Al, Na and Si, which are mainly from the silicate nanoclay, were detected indicating that the nanoclay had been successfully incorporated into the composite (Cai, Riedl, Zhang, & Wan, 2008).

5.5. Mechanical property study

The flexural and tensile properties of composites with varying percentage of glutaraldehyde and clay are shown in Table 2. The values shown in the table are the mean values of five readings. It was observed that both the flexural and tensile modulus and strength increased with the increase in the concentration of glutaraldehyde. The increase in mechanical properties could be ascribed to the formation of crosslinking between the polar groups of starch and jute by glutaraldehyde as shown in Fig. 1(B). The mechanical properties of composite were found to increase with the increase in the concentration of GA (Ramaraj, 2007). It was observed from Table 2 that except the flexural strength there was no significant enhancement on the properties such as flexural modulus, tensile strength and tensile modulus beyond 50% of GA. This might be due to saturation of crosslinking sites in both starch and jute surface. Since, all these properties together culminate to the overall mechanical strength of the composite. Hence, considering the 50% concentration of the crosslinker as optimum, we modified the composite (S/J/G50/M1, S/J/G50/M3 and S/J/G50/M5) with different percentage of nanoclay ranging from 1 to 5% (w/w) of starch. The mechanical properties of the clay treated samples were found better compared to the clay untreated samples. The higher the percentage of clay, the higher was the mechanical properties. The increase in mechanical properties was due to the restriction in the mobility of the intercalated polymer chains present inside the silicate layers of clay (Becker, Cheng, Varley, & Simon, 2003).

5.6. Thermal property study

The influence of crosslinker and nanoclay on the thermal properties of the synthesized composites was investigated by TGA, as shown in Fig. 4(A). Table 3 (derived from Fig. 4(A)) shows the initial decomposition temperature (T_i), maximum pyrolysis temperature (T_m), decomposition temperature (T_D) at different weight loss (%) and residual weight (RW) of the composites. It was seen clearly from the thermograms that the T_i, T_m, T_D at different weight loss (%) and residual weight (RW, %) were improved with the addition of crosslinker.

T_i values of S/J composites were found to enhance with the increase in the percentage of crosslinker concentration. T_i values increased further due to incorporation of clay. The interesting area of TGA of starch based composite is the 250–350 °C temperature range. T_m values for both the stages of pyrolysis were found to increase as the percentage of crosslinker increased. T_D values of the crosslinked S/J composite were higher than uncrosslinked S/J composite. The higher the crosslinker concentration, the higher was the T_D value. This might be due to the formation of crosslinking caused by the interaction between glutaraldehyde and different polar groups present in starch and jute. The T_D values were improved further when clay was added to it. The increase in thermal stability of the synthesized nanocomposites is attributed to the hindered diffusion of volatile decomposition products within it (Gilman et al., 2000). This might also be due to the physico-chemical adsorption of the volatile degradation products on the silicate surface (Zanetti, Camino, Reichert, & Mulhaupt, 2001). The volatilization of the degraded products originated by carbon—carbon bond scission in the composite was delayed by tortuous path provided by the silicates layer (Qin et al., 2004). Clay treated composite showed a subsidiary increase in RW values over clay untreated composite. Therefore, it could be concluded that the thermal stability of the S/J composites increased on addition of crosslinker and nanoclay.

5.7. LOI study

The LOI values of the S/J composites with different percentage of crosslinker and clay are presented in the Table 4. From that table, it was observed that LOI value increased with the increase in the percentage of crosslinker. GA formed crosslinks between jute and starch. The higher the concentration of GA, the

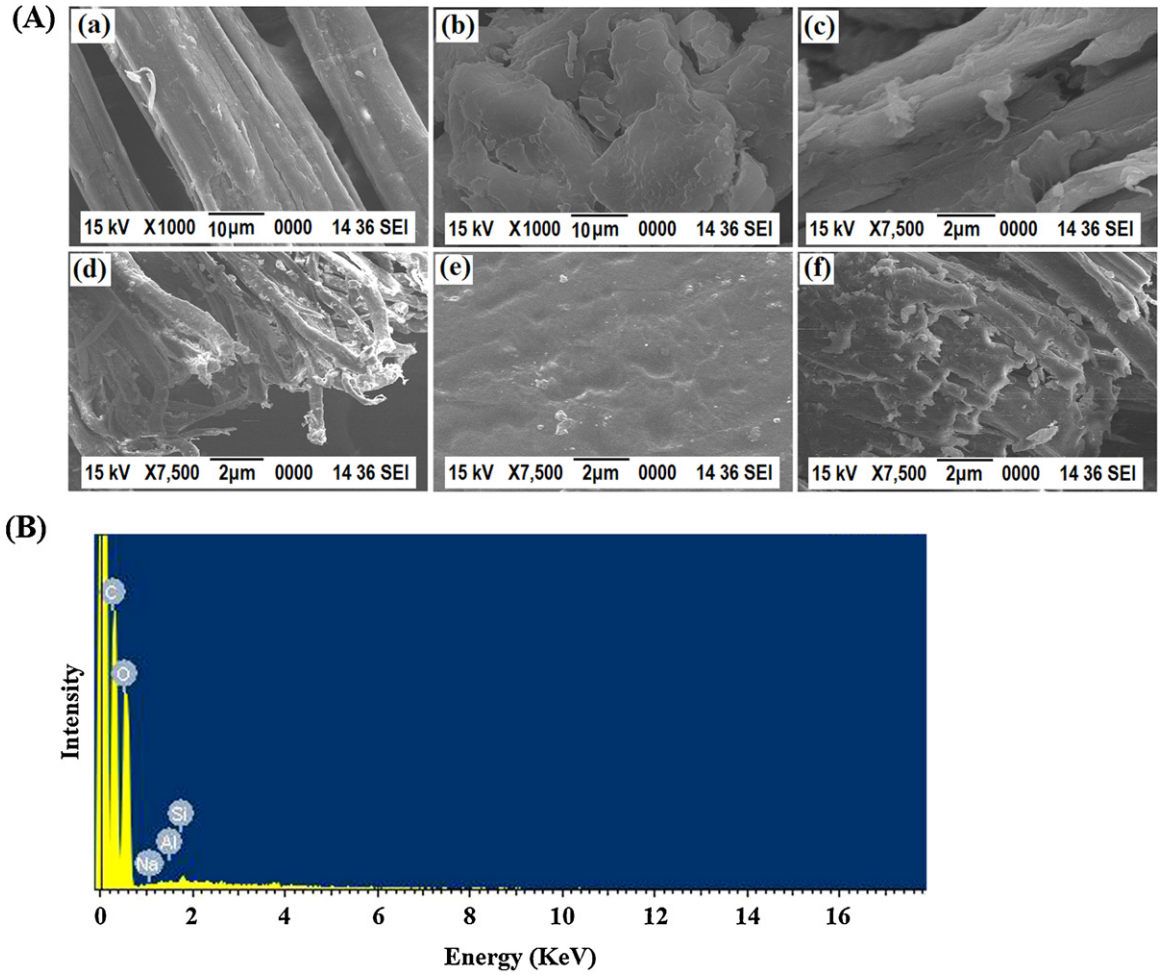

Fig. 3. (A) SEM micrographs of (a) jute, (b) starch, (c) S/J/G50 smooth surface, (d) S/J/G50 fracture surface, (e) S/J/G50/M5 smooth surface, (f) S/J/G50/M5 fracture surface. (B) Energy dispersive X-ray analysis of S/J/G50/M.

Table 2
Flexural and tensile properties of (a) S/J, (b) S/J/G30, (c) S/J/G40, (d) S/J/G50, (e) S/J/G60, (f) S/J/G70, (g) S/J/G50/M1, (h) S/J/G50/M3 and (i) S/J/G50/M5.[a]

Sample	Flexural properties		Tensile properties	
	Strength (MPa)	Modulus (MPa)	Strength (MPa)	Modulus (MPa)
S/J	27.67 (±1.22)	1141.9 (±1.57)	12.59 (±1.26)	755.38 (±16.74)
S/J/G30	28.31 (±1.34)	1336.2 (±1.16)	18.62 (±1.84)	1117.10 (±13.46)
S/J/G40	37.8 (±2.31)	1641.6 (±2.11)	19.88 (±0.96)	1192.53 (±17.32)
S/J/G50	39.5 (±2.14)	2234.0 (±1.96)	22.54 (±1.03)	1352.18 (±15.34)
S/J/G60	45.8 (±1.12)	2575.6 (±1.32)	22.65 (±1.31)	1358.81 (±10.79)
S/J/G70	51.4 (±1.32)	2620.1 (±1.13)	24.64 (±2.07)	1478.53 (±14.08)
S/J/G50/M1	69.8 (±1.31)	3777.0 (±2.09)	28.42 (±0.74)	1705.47 (±11.67)
S/J/G50/M3	82.0 (±1.76)	4516.3 (±1.54)	32.40 (±1.37)	1944.78 (±17.62)
S/J/G50/M5	90.7 (±2.54)	6434.1 (±2.09)	40.53 (±2.31)	2344.67 (±12.78)

[a] Each value represents average five samples.

Table 3
Thermal properties of starch, jute, glutaraldehyde and nanoclay composite.[a]

Sample particulars	T_i	$^{I}T_m$	$^{II}T_m$	Temperature of decomposition at different weight loss (%)						RW % at 600 °C
				20	30	40	50	60	70	
S/J	176 ± 1	220 ± 1	321 ± 2	283 ± 1	305 ± 2	315 ± 1	325 ± 1	334 ± 2	350 ± 2	10 ± 1
S/J/G30	182 ± 2	319 ± 1	360 ± 1	287 ± 2	308 ± 1	318 ± 2	326 ± 1	335 ± 1	354 ± 1	13 ± 1
S/J/G50	196 ± 1	322 ± 2	365 ± 2	291 ± 1	309 ± 1	319 ± 1	327 ± 1	338 ± 1	355 ± 2	15 ± 2
S/J/G70	197 ± 2	324 ± 2	366 ± 1	296 ± 2	310 ± 2	320 ± 1	328 ± 1	340 ± 2	357 ± 1	16 ± 2
S/J/G50/M1	218 ± 1	351 ± 1	391 ± 2	298 ± 1	313 ± 1	322 ± 1	331 ± 1	341 ± 2	361 ± 1	18 ± 2
S/J/G50/M3	219 ± 2	354 ± 2	393 ± 1	299 ± 1	314 ± 1	323 ± 2	332 ± 1	341 ± 2	361 ± 1	20 ± 1
S/J/G50/M5	221 ± 2	359 ± 1	397 ± 1	301 ± 2	316 ± 1	325 ± 1	334 ± 1	344 ± 2	364 ± 1	23 ± 2

T_i: initial decomposition temperature; $^{I}T_m$: maximum pyrolysis temperature value for 1st step; $^{II}T_m$: maximum pyrolysis temperature value for 2nd step.
[a] Each value represents average three samples.

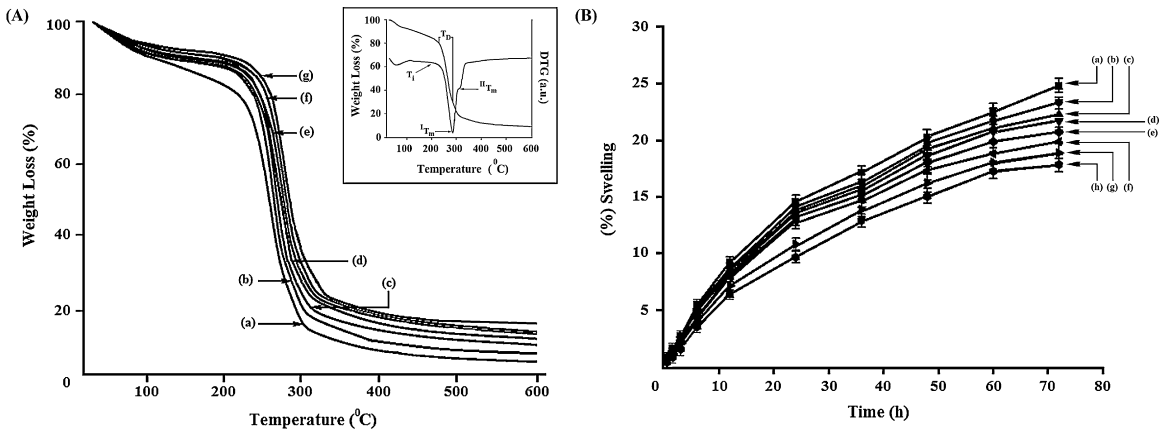

Fig. 4. (A) TGA thermograms of (a) S/J, (b) S/J/G30, (c) S/J/G50, (d) S/J/G70, (e) S/J/G50/M1, (f) S/J/G50/M3 and (g) S/J/G50/M5. TGA and DTG for curve (c) are shown in the inset. (B) Swelling behaviour of (a) S/J, (b) S/J/G30, (c) S/J/G40, (d) S/J/G50, (e) S/J/G70, (f) S/J/G50/M1, (g) S/J/G50/M3 and (h) S/J/G50/M5.

Table 4
Limiting oxygen indices (LOI) and Flaming characteristics of the prepared composites.[a]

Samples	LOI (%)	Flame description	Smoke and fumes	Char
S/J	22 (±2.0)	Candle like Flame	Small and black smoke	Little
S/J/G30	29 (±1.0)	Small localised flame	Small and black smoke	Little
S/J/G40	38 (±3.0)	Small localised flame	Small and black smoke	Little
S/J/G50	39 (±1.0)	Small localised flame	Small and black smoke	Little
S/J/G60	44 (±2.0)	Small localised flame	Small and black smoke	Little
S/J/G70	47 (±1.0)	Small localised flame	Small and black smoke	Little
S/J/G50/M1	51 (±2.0)	Small localised flame	Small and black smoke	Higher
S/J/G50/M3	56 (±3.0)	Small localised flame	Small and black smoke	Higher
S/J/G50/M5	61 (±2.0)	Small localised flame	Small and black smoke	Higher

[a] Each value represents average five samples.

higher is the crosslinking (Ramaraj, 2007). The network structure thus formed would restrict the accessibility of oxygen for the production of degradable components from the composites and hence LOI value would be more. LOI value was enhanced further on addition of nanoclay. The LOI values of the nanoclay treated composites were found more compared to nanoclay untreated composite. The higher the percentage of nanoclay, the higher was the LOI value. Jute, primarily composed of plant materials cellulose and lignin, requires a very less amount of oxygen for the production of flammable volatiles and propagation of flame and hence showed very low LOI value. Whereas, the incorporation of the nanoclay particle into the synthesized composite produced a silicate char on the surface of it and hence improved their flame resistance property (Urbanczyk et al., 2010). The silicate rich surface had better barrier property to heat and oxygen transport due to which ignition of the composite delayed. Therefore, with increase in the concentration of clay, the resistance of flame propagation was improved and hence higher LOI values were observed.

5.8. Dimensional study

The effect of swelling in water vapour at room temperature (∼30° C) and 65% relative humidity for the composite samples for different time periods is shown in Fig. 4(B). In all the cases, the % swelling was found to increase with the increase of time. From the figure, it was observed that the composites having higher percentage of GA showed more reduction in swelling than the composites containing lower percentage of GA (Das et al., 2010). Composites containing higher percentage of GA swelled less due to higher crosslink densities and less availability of the polar groups. Clay treated composites swelled less than those of clay untreated samples. The higher the amount of clay, the lower was the swelling. The silicate layer of clay provided a tortuous path which hindered the diffusivity of water through the composites (Rana, Gupta, Rao, & Sridhar, 2005).

6. Conclusion

Environmental-friendly composites made of jute fabric and starch matrix, plasticized with glycerol, were prepared by solution induced intercalation method and characterized by various techniques. Effect of the crosslinking agent, GA and the nanoclay particles were studied. The incorporation of the crosslinking agent improved the physicochemical properties such as mechanical, thermal, flame retardancy and dimensional stability via the interaction of the aldehydic group of the crosslinker with the hydroxyl group of starch and jute. The optimum concentration of GA for obtaining overall improvement in mechanical properties of the synthesized composites was found to be 50%. FTIR study showed a strong interaction among jute fabric, starch, glutaraldehyde and nanoclay. XRD and TEM study showed the exfoliation of nanoclay in the composites. The various properties such as mechanical, thermal, flame retardancy and dimensional stability were found to improve further by the incorporation of the nanoclay to the resultant composites. The adherence of starch and clay particles on the surface of the jute fibre was shown by SEM study. SEM study of fractured surfaces also revealed the intimate bonding between the jute fabric and the matrix material. Therefore, such kind of nanoclay loaded jute fabric reinforced starch composites are eco-friendly and can find applications in newer fields.

Polymeric materials offer new possibilities and challenges, for all types of materials having the capability to replace different classes such as metallic, ceramic and wood with the combination of different properties in the form of composites/nanocomposites. In recent years the “green nanocomposites” have made their own domain in the field of sustainable development. Most importantly,

the green nanocomposites especially of those prepared by using naturally available resources have contributed to an extent in replacing the conventional materials. These green nanocomposites have the potential for a wider application range such as computer casings, packaging and panels for auto interior. Therefore, these synthesized plant based composites/nanocomposites having optimised properties may add to the rapid development for more sustainable and ecofriendly materials in near future.

Acknowledgement

Financial support for this study from Department of Science and Technology (SR/S5/GC-13/2008), New Delhi is gratefully acknowledged.

References

Aboubakar, Njintang, Y. N., Scher, J., & Mbofung, C. M. F. (2008). Physicochemical, thermal properties and microstructure of six varieties of taro (*Colocasia esculenta* L. Schott) flours and starches. *Journal of Food Engineering*, *86*(2), 294–305.

Ban, W., JianguoSong, Argyropoulos, D. S., & Lucia, L. A. (2006). Improving the physical and chemical functionality of starch derived films with biopolymers. *Journal of Applied Polymer Science*, *100*(3), 2542–2548.

Bastioli, C. (1995). In G. Scott, & D. Gillead (Eds.), *Starch polymer composites in degradable polymers principles and applications*. London: Chapman and Hall (Chapter 6).

Becker, O., Cheng, Y. B., Varley, R. J., & Simon, G. P. (2003). Layered silicate nanocomposites based on various high-functionality epoxy resins: The influence of cure temperature on morphology, mechanical properties, and free volume. *Macromolecules*, *36*(5), 1616–1625.

Bondeson, D., Mathew, A., & Oksman, K. (2006). Optimization of the isolation of nanocrystals from microcrystalline cellulose by acid hydrolysis. *Cellulose*, *13*(2), 171–180.

Cai, X., Riedl, B., Zhang, S. Y., & Wan, H. (2008). The impact of the nature of nanofillers on the performance of wood polymer nanocomposites. *Composites Part A: Applied Science and Manufacturing*, *39*(5), 727–737.

Chen, G. Q., & Patel, M. K. (2012). Plastics derived from biological sources: Present and future: A technical and environmental review. *Chemical Reviews*, doi:org/10.1021/cr200162d.

Chen, P., & Zhang, L. (2006). Interaction and properties of highly exfoliated soy protein/montmorillonite nanocomposites. *Biomacromolecules*, *7*(6), 1700–1706.

Corre, D. L., Bras, J., & Dufresne, A. (2010). Starch nanoparticles: A review. *Biomacromolecules*, *11*(5), 1139–1153.

Das, K., Ray, D., Bandyopadhyay, N. R., Gupta, A., Sengupta, S., Sahoo, S., et al. (2010). Preparation and characterization of cross-linked starch/poly(vinyl alcohol) green films with low moisture absorption. *Industrial and Engineering Chemical Research*, *49*(5), 2176–2185.

Deka, B. K., & Maji, T. K. (2011). Study on the properties of nanocomposite based on high density polyethylene, polypropylene, polyvinyl chloride and wood. *Composites Part A: Applied Science and Manufacturing*, *42*(6), 686–693.

Dufrense, A., & Vignon, M. R. (1998). Improvement of starch film performances using cellulose microfibrils. *Macromolecules*, *31*(8), 2693–2696.

Fishman, M. L., Coffin, D. R., Konstance, R. P., & Onwulata, C. I. (2000). Extrusion of pectin/starch blends plasticized with glycerol. *Carbohydrate Polymers*, *41*(4), 317–325.

Forssell, P. M., Mikkilä, J. M., Moates, G. K., & Parker, R. (1997). Phase and glass transition behaviour of concentrated barley starch–glycerol–water mixtures, a model for thermoplastic starch. *Carbohydrate Polymers*, *34*(4), 275–282.

Gao, W., Dong, H., Hou, H., & Zhang, H. (2012). Effects of clays with various hydrophilicities of starch–clay nanocomposites by film blowing. *Carbohydrate Polymers*, *88*(1), 321–328.

Gilman, J. W., Jackson, C. L., Morgan, A. B., Harris, R., Manias, E., Gannelis, E. P., et al. (2000). Flammability properties of polymer layered-silicate nanocomposites. Polypropylene and polystyrene nanocomposites. *Chemistry of Materials*, *12*(7), 1866–1873.

Hillberg, A. L., Holmes, C. A., & Tabrizian, M. (2009). Effect of genipin cross-linking on the cellular adhesion properties of layer-by-layer assembled polyelectrolyte films. *Biomaterials*, *30*(27), 4463–4470.

Huang, X., & Netravali, A. N. (2006). Characterization of nano-clay reinforced phytagel-modified soy protein concentrate resin. *Biomacromolecules*, *7*(10), 2783–2789.

Jahan, M. S., Saeed, A., He, Z., & Ni, Y. (2011). Jute as raw material for the preparation of microcrystalline cellulose. *Cellulose*, *18*(2), 451–459.

Kvien, I., Sugiyama, J., Votrubec, M., & Oksman, K. (2007). Characterization of starch based nanocomposites. *Journal of Materials Science*, *42*(19), 8163–8171.

Liu, H., Chaudhary, D., Yusa, S., & Tade, M. O. (2011). Glycerol/Starch/Na^+–montmorillonite nanocomposites: A XRD, FTIR, DSC and ^1H NMR study. *Carbohydrate Polymers*, *83*(4), 1591–1597.

Lu, W. H., Zhao, G. J., & Xue, Z. H. (2006). Preparation and characterization of wood/montmorillonite nanocomposites. *Forestry Studies in China*, *8*(1), 35–40.

Ma, X., Yu, J., & Kennedy, J. F. (2005). Studies on the properties of natural fibres-reinforced thermoplastic starch composites. *Carbohydrate Polymers*, *62*(1), 19–24.

Mitsudome, T., Matsuno, T., Sueoka, S., Mizugaki, T., Jitsukawa, K., & Kaneda, K. (2012). Direct synthesis of unsymmetrical ethers from alcohols catalyzed by titanium cation-exchanged montmorillonite. *Green Chemistry*, doi:10.1039/c2gc16135d.

Pandey, J. K., & Singh, R. P. (2001). UV irradiated biodegradability of ethylene–propylene copolymers, LDPE and i-PP in composting and culture environments. *Biomacromolecules*, *2*(3), 880–885.

Plackett, D., Anderson, T. L., Pedersen, W. B., & Nielson, L. (2003). Biodegradable composites based on L-polylactide and jute fibres. *Composite Science and Technology*, *63*(9), 1287–1296.

Qin, H., Zhang, S., Zhao, C., Feng, M., Yang, M., Shu, Z., et al. (2004). Thermal stability and flammability of polypropylene/montmorillonite composites. *Polymer Degradation and Stability*, *85*(2), 807–813.

Ramaraj, B. (2007). Crosslinked poly (vinyl alcohol) and starch composite films. II. Physicomechanical, thermal properties and swelling studies. *Journal of Applied Polymer Science*, *103*(2), 909–916.

Rana, H. T., Gupta, R. K., Rao, H. V. S. G., & Sridhar, L. N. (2005). Measurement of moisture diffusivity through layered-silicate nanocomposites. *AIChE Journal*, *51*(12), 3249–3256.

Ray, S. S., & Okamoto, M. (2003). Polymer/layered silicate nanocomposites: A review from preparation to processing. *Progress in Polymer Science*, *28*(11), 1539–1641.

Ray, D., & Sarkar, B. K. (2001). Characterization of alkali-treated jute fibres for physical and mechanical properties. *Journal of Applied Polymer Science*, *80*(7), 1013–1020.

Ray, D., Sengupta, S., Sengupta, S. P., Mohanty, A. K., & Misra, M. (2007). A study of the mechanical and fracture behavior of jute fabric reinforced clay modified thermoplastic starch-matrix composites. *Macromolecular Materials and Engineering*, *292*(10–11), 1075–1084.

Saha, A. K., Das, S., Basak, R. K., Bhatta, D., & Mitra, B. C. (2000). Improvement of functional properties of jute-based composite by acrylonitrile pretreatment. *Journal of Applied Polymer Science*, *78*(3), 495–506.

Saheb, D. N., & Jog, J. P. (1999). Natural fibre polymer composites: A review. *Advances in Polymer Technology*, *18*(4), 351–363.

Satyanarayana, K. G., Arizaga, G. G. C., & Wypych, F. (2009). Biodegradable composites based on lignocellulosic fibres—An overview. *Progress in Polymer Science*, *34*(9), 982–1021.

Scott, G. (2000). Green polymers. *Polymer Degradation and Stability*, *68*(1), 1–7.

Shogren, R. L., Fanta, G., & Doanne, W. M. (1993). Development of starch based plastics—A re-examination of selected polymer systems in historical perspective. *Starch/Stańke*, *45*(8), 276–280.

Sukitpaneenit, P., & Chung, T. S. (2012). PVDF/nanosilica dual-layer hollow fibers with enhanced selectivity and flux as novel membranes for ethanol recovery. *Industrial & Engineering Chemistry Research*, *51*(2), 978–993.

Urbanczyk, L., Bourbigot, S., Calberg, C., Detrembleur, C., Jerome, C., Boschini, F., et al. (2010). Preparation of fire-resistant poly (styrene-co-acrylonitrile) foams using supercritical CO_2 technology. *Journal of Materials Chemistry*, *20*(8), 1567–1575.

Yoonessi, M., Toghiani, H., Kingery, W. L., & Pittman, C. U., Jr. (2004). Preparation, characterization, and properties of exfoliated/delaminated organically modified clay/dicyclopentadiene resin nanocomposites. *Macromolecules*, *37*(7), 2511–2518.

Zanetti, M., Camino, G., Reichert, P., & Mulhaupt, R. (2001). Thermal behavior of poly(propylene) layered silicate nanocomposites. *Macromolecular Rapid Communications*, *22*(3), 176–180.

Zhang, C., Tjiu, W. W., Fan, W., Yang, Z., Huang, S., & Liu, T. (2012). Aqueous stabilization of graphene sheets using exfoliated montmorillonite nanoplatelets for multifunctional free-standing hybrid films via vacuum-assisted self-assembly. *Journal of Materials Chemistry*, doi:10.1039/c1jm13236a.